CHAPTER 11

Alaska: Glaciers of Kenai Fjords National Park and Katmai National Park and Preserve

Bruce A. Giffen, Dorothy K. Hall, and Janet Y.L. Chien

ABSTRACT

There are hundreds of glaciers in Kenai Fjords National Park (KEFJ) and Katmai National Park and Preserve (KATM) covering over 2,276 km^2 of park land (ca. 2000). There are two primary glacierized areas in KEFJ (the Harding Icefield and the Grewingk-Yalik Glacier Complex) and three primary glacierized areas in KATM (the Mt. Douglas area, the Kukak Volcano to Mt. Katmai area, and the Mt. Martin area). Most glaciers in these parks terminate on land, though a few terminate in lakes. Only KEFJ has tidewater glaciers, which terminate in the ocean. Glacier mapping and analysis of the change in glacier extent has been accomplished on a decadal scale using satellite imagery, primarily Landsat data from the 1970s, 1980s, and from 2000. Landsat Multispectral Scanner (MSS), Thematic Mapper (TM), and Enhanced Thematic Mapper Plus (ETM+) imagery was used to map glacier extent on a park-wide basis. Classification of glacier ice using image-processing software, along with extensive manual editing, was employed to create Geographic Information System (GIS) outlines of the glacier extent for each park. Many glaciers that originate in KEFJ but terminate outside the park boundaries were also mapped. Results of the analysis show that there has been a reduction in the amount of glacier ice cover in the two parks over the study period. Our measurements show a reduction of approximately 21 km^2, or −1.5% (from 1986 to 2000), and 76 km^2, or −7.7% (from 1986/1987 to 2000), in KEFJ and KATM, respectively. This work represents the first comprehensive study of glaciers of KATM. Issues that complicate the mapping of glacier extent include debris cover (moraine and volcanic ash), shadows, clouds, fresh snow, lingering snow from the previous season, and differences in spatial resolution between the MSS, TM, or ETM+ sensors. Similar glacier mapping efforts in western Canada estimate mapping errors of 3–4%. Measurements were also collected from a suite of glaciers in KEFJ and KATM detailing terminus positions and rates of recession using datasets including 15 min USGS quadrangle maps (1950/1951), Landsat imagery (1986/1987, 2000, 2006), and 2005 IKONOS imagery (KEFJ only).

11.1 INTRODUCTION

Glaciers represent a significant landcover type in Kenai Fjords National Park (KEFJ) and Katmai National Park and Preserve (KATM), about 50% and 5% by area, respectively. Any change in this landcover type will have impacts on the ecosystems and hydrology of these parks. The glaciers are also intricately related to climate and are indicators of regional climate change. In general, land-based glaciers are known to be responsive to short-term

J. S. Kargel et al. (eds.), *Global Land Ice Measurements from Space*, Springer Praxis Books,
DOI: 10.1007/978-3-540-79818-7_11,

climate change (however, there are many exceptions to this; Hall et al. 2005). Tidewater glaciers are known to have an ice marginal fluctuation cycle that is not necessarily directly related to short-term climate change (Meier and Post 1987). Glaciers also influence local climate because of their high reflectivity. Alaskan glaciers are also important contributors to global sea level rise (Dyurgerov and Meier 1997, Arendt et al. 2002). To improve our understanding of the extent and rate of change of the glacier terminus and margin changes, an effort to map the glacier extent on a decadal scale was initiated in the National Park Service's (NPS) Southwest Alaska Network (SWAN), which consists of the following parks: KEFJ, KATM, Lake Clark National Park and Preserve, Aniakchak National Monument and Preserve, and the Alagnak National Wild River. Glacier extent mapping has been completed in KEFJ and KATM. This work is part of the long-term Inventory and Monitoring (I&M) Program of the NPS. The goals of the I&M Program are to collect, organize, and make available natural resource data to park management and staff, the scientific community, and the public, and to further the knowledge and understanding of natural resources and ecosystem function in national parks.

Glaciers throughout KEFJ have been in widespread recession since the Little Ice Age maxima (late 1700s through late 1800s) (Wiles 1992). There are no detailed studies documenting the behavior of KATM glaciers. The goal for this project was to map the glacier ice extent on a park-wide basis on a decadal scale beginning in the 1970s using multispectral satellite imagery to permit quantification of park-wide change in total area of glacier ice and to identify trends and areas of rapid glacier ice extent change. Landsat satellite–based instrumentation was selected to be the primary tool for this work because its spatial, spectral, and temporal resolution is well suited for the objectives of the project, and because of its decades-long data record availability.

Prior to this mapping effort, the only region-wide glacier mapping data available for KEFJ and KATM was the glacier ice/permanent snowfield landscape cover type estimate from the Alaska-wide hydrography dataset. This dataset was created by the U.S. Geological Survey (USGS) and the Bureau of Land Management (BLM) by updating the USGS digital line graphs (1:63,360 scale, ca. 1950s) using the Alaska High Altitude Aerial Photography (AHAP) image database (late 1970s through mid-1980s). This Alaska-wide hydrography dataset (ca. 1980s) shows that glaciers and permanent snowfields covered 1,398 km^2 in KEFJ and 994 km^2 in KATM.

The extent of icefields and glaciers in KEFJ and KATM was mapped using the Landsat Multispectral Scanner (MSS) (79 m pixel resolution), first launched in 1972; Thematic Mapper (TM) (30 m pixel resolution), first launched in 1982; and Enhanced Thematic Mapper Plus (ETM+) (up to 15 m pixel resolution), launched in 1999. Geographic Information System (GIS) vector outlines were produced which can also be used in future analyses to measure changes, and to compare areal extent and terminus positions of glaciers in these parks.

The interpretation of Landsat data was supplemented with the use of AHAP, flown during the late 1970s through the mid-1980s at a scale of approximately 1:65,000. Additionally, experience and local knowledge gained from fieldwork within the project area were used in the mapping effort. In KEFJ, IKONOS imagery (1 m pixel resolution) was used to augment the mapping of glacier terminus positions for a few selected glaciers throughout the park.

Changes in glacier terminus position and rates of recession were determined using 15 min USGS quadrangle maps (derived from high-quality aerial photography—1950/1951), Landsat imagery (1986, 1987, 2000, 2006; KEFJ only), and 2005 IKONOS imagery (KEFJ only).

11.2 REGIONAL CONTEXT

11.2.1 Geographic/topographic/environmental setting

Located on the North American Plate, both KATM and KEFJ lie along the convergent tectonic plate boundary where the oceanic Pacific Plate is subducting beneath the mélange of terrains and accretionary complexes that comprise the Alaska portion of the North American Plate. KATM and the surrounding region are underlain by a broad northeast-trending volcanic complex, directly coupled with and orthogonal to the Aleutian subduction trench; KATM contains at least 17 active volcanoes (Bennett et al. 2006) with elevations up to 2,300 m. The Aleutian Trench is located 350 km southeast of the Katmai volcanic front. Though not volcanic, the mountains of KEFJ rise abruptly from sea level to >1,800 m asl.

11.2.2 Climate

These two parks are aligned along the northern coast of the Gulf of Alaska where the climate is dominated by maritime influences. This region experiences a high frequency of marine cyclones, many of which make landfall in some of the most geographically and geologically extreme and dramatic terrain in North America. Important features of the climate–hydrological cycle in these parks include the location of the Aleutian Low (a persistent center of atmospheric low pressure) during the winter months (Davey et al. 2007) and the presence of mountains rising abruptly and steeply from the Gulf of Alaska (Bennett et al. 2006, Davey et al. 2007). Maritime climate influences interact with steep topography to create patterns of high precipitation on the windward side of the mountains, and rain shadows on the leeward side; regional winds have an easterly component (Davey et al. 2007), and dominate during the winter and common during the summer. The majority of winter precipitation (snow and ice) typically occurs October through April in these parks (KATM and KEFJ).

Generally, KATM is cooler and drier than KEFJ, based on PRISM (Parameter-elevation Regression on Independent Slopes Model) temperature and precipitation models (Daly et al. 1994, 2002), though there are no long-term climate records at high elevations that are proximal to the project areas with which to verify the PRISM models. Climate records from weather stations proximal to KATM and KEFJ come from King Salmon and Seward, Alaska, respectively. Based on climate records—the dataset of climate normals produced by the National Climatic Data Center (NCDC)—at King Salmon and Seward, Alaska (1961–1990 and 1971–2000), the annual monthly mean temperature climate normal at both of these sites has increased 0.5 and 0.3°C, respectively. King Salmon's annual monthly mean temperature climate normal is 1.3°C and Seward's annual monthly mean temperature climate normal is 4.6°C (NCDC, 1971–2000). King Salmon's annual monthly mean precipitation climate normal is 493 mm and Seward's annual monthly mean precipitation climate normal is 1,824 mm (NCDC, 1971–2000). It should be noted that the King Salmon climate data (National Weather Service Cooperative weather station #504766-6), and the Seward climate data (Coop weather station #508371-2), are located at low elevations (15 and 12 m asl, respectively). Also note the Seward Coop weather station is on the windward side of the mountains whereas the King Salmon Coop weather station is on the leeward side, thus explaining the dramatic divergence in annual precipitation observed between the two stations. Long-term climate-monitoring stations in remote Alaskan locations at higher elevations are uncommon.

11.2.3 Glacier characteristics—Kenai Fjords National Park

Harding Icefield and the Grewingk-Yalik Glacier Complex are predominately located within KEFJ (Fig. 11.1 and Online Supplement 11.1) spawning dozens of outlet valley glaciers. Fourteen glaciers in KEFJ are named. An excellent introduction to these icefields may be found in Field (1975).

The Harding Icefield is located on the southeast side of the Kenai Peninsula, with icefield elevations reaching 1,500 m asl. The icefield is approximately 80×30 km in area and spawns several dozen outlet glaciers that flow down valleys and terminate on land, in lakes, or in the Gulf of Alaska. Some valley glaciers coalesce into larger valley glaciers.

A few kilometers to the southwest of the Harding Icefield is the Grewingk-Yalik Glacier Complex with elevations reaching 1,400 m asl. This accumulation of glacier ice is approximately 35×10 km in area, and spawns several outlet valley glaciers that terminate on land and in lakes. There are no tidewater glaciers issuing from the Grewingk-Yalik Glacier complex.

The mean ice elevation of the glacierized area of Harding Icefield and the Grewingk-Yalik Glacier Complex is 970 m asl and approximately 59% of the glacierized area has a surface slope of 20° or less (based on the USGS National Elevation Dataset, 1999).

Glacier termini characteristics include typical clean ice boundaries of calving tidewater or lake-terminating glaciers. Many termini of land-terminating glaciers of the Harding Icefield and the Grewingk-Yalik Glacier Complex are covered in varying amounts of moraine material. The larger valley glaciers are striped with characteristic medial moraines as a result of coalescing valley glaciers; these valley glaciers also exhibit large accumulations of lateral moraine material on the glacier surface. There are isolated cirque glaciers and small valley glaciers issuing from simple and compound basins beyond the main confines of the Harding Icefield and Grewingk-Yalik Glacier Complex.

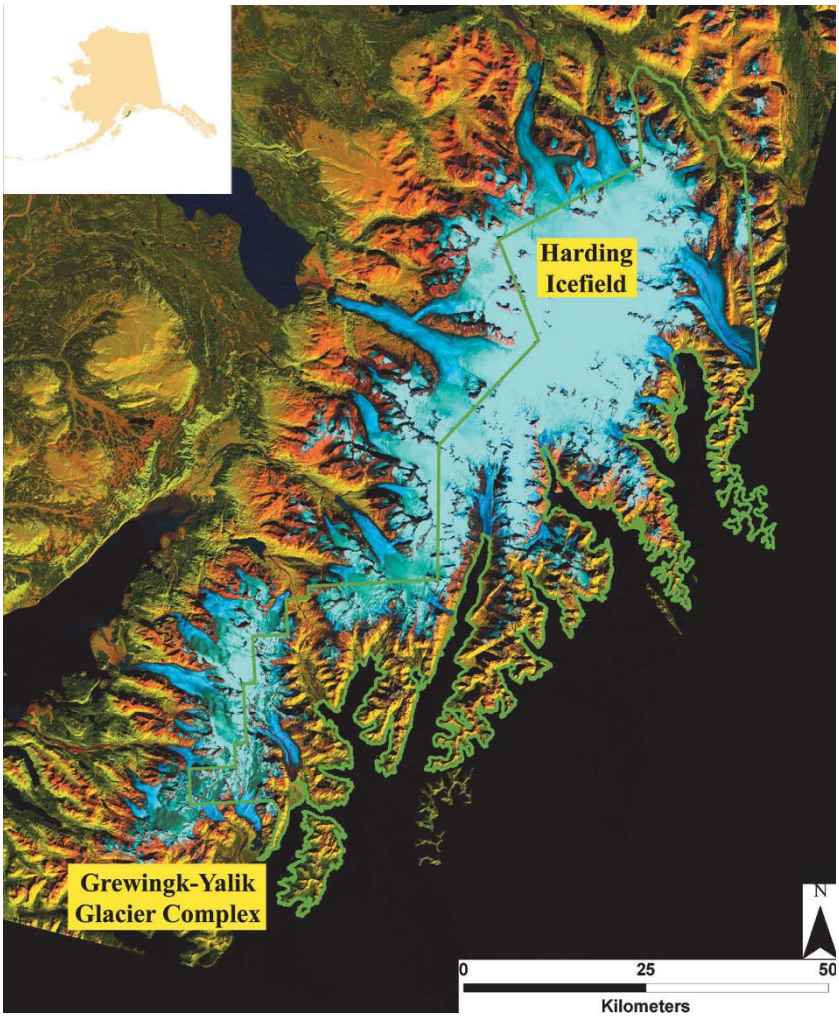

Figure 11.1. Landsat satellite color composite image of the Harding Icefield and the Grewingk-Yalik Glacier Complex with the KEFJ park boundary shown. The inset identifies the location of KEFJ in reference to Alaska (Landsat TM5, September 12, 1986; 542 RGB). See Online Supplement 11.1 for high-resolution version.

Innumerable small isolated permanent snowfields also occur at higher elevations beyond the limits of glacier ice.

The Harding Icefield was the focus of extensive work during the 1990s (Echelmeyer et al. 1996, Adalgeirsdóttir et al. 1998, Sapiano et al. 1998, Arendt et al. 2002). Echelmeyer et al. (1996) used airborne altimetry to generate elevation profiles along the centerlines of main glacier trunks and major tributaries and compared these profiles with contours on 15 min USGS quadrangle maps derived from aerial photographs acquired in the 1950s. They estimated that total volume change for the Harding Icefield for this ~43-year period was 34 km^3, which corresponds to an area average glacier surface elevation change of -21 ± 5 m. Hall et al. (2005) provided preliminary mapping results of KEFJ, showing a general recession of the glaciers in and near KEFJ.

11.2.4 Glacier characteristics—Katmai National Park and Preserve

KATM is located on the northern extent of the Alaska Peninsula. There are over 50 glaciers within the boundaries of KATM originating from three primary areas of accumulation (Fig. 11.2 and Online Supplement 11.2). Each of these areas is a center of volcanic activity with elevations approaching 2,300 m asl, and each area spawns many valley glaciers, the most common glacier type in KATM. Many of the larger valley glaciers origin-

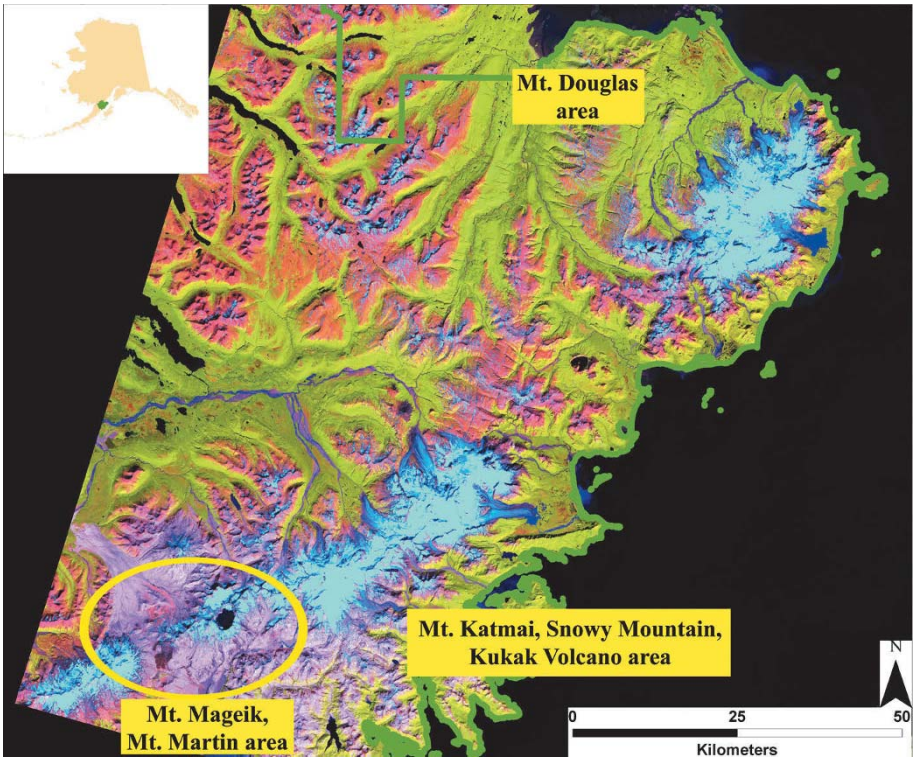

Figure 11.2. Landsat satellite color composite image of glacierized areas in KATM. The inset identifies the location of KATM in reference to Alaska (Landsat ETM+, August 16, 2000; 542 RGB). Figure can also be viewed in higher resolution as Online Supplement 11.2.

ate from compound basins coalescing into larger valley glaciers. Most of KATM's glaciers terminate on land with a few terminating in lakes. The mean ice elevation of the glacierized area of KATM is 1,210 m and approximately 24% of the glacierized area has a surface slope of 20° or less (based on the USGS National Elevation Dataset, 1999). Generally, the glacierized terrain here is much steeper than that found in KEFJ. Beyond the three primary accumulations of glacier ice on these volcanic mountains, there are small cirque glaciers and innumerable small isolated permanent snowfields. Only seven glaciers in KATM are named.

There are no tidewater glaciers in KATM; however, there are two large lake-terminating glaciers exhibiting clean ice boundaries. Most glacier termini in KATM have a significant amount of moraine cover. The larger valley glaciers of KATM have confluent tributary relationships with other valley glaciers, exhibited by significant accumulations of medial moraine material on glacier surfaces. In addition, since the volcanic eruption of Novarupta in 1912, vast exposures of volcanic ash remain (Figs. 11.2 and 11.3). Frequent wind events in the area entrain volcanic ash and redeposit this ash over the landscape. Subsequently, many glaciers in this portion of KATM are completely blanketed with a thick layer of volcanic ash (Fig. 11.3).

Very little work has been done on the glaciers of KATM, and even fewer publications are in the open literature. Field (1975) provided a map of the area with some background, and Motyka (1977) documented observations of glacier growth within the Katmai Caldera. Our present work thus documents an important group of glaciers that has not been well studied.

11.3 PROCEDURES FOR ANALYSIS OF GLACIER CHANGES

11.3.1 Imagery classification

Initially, Landsat imagery was acquired that met the following standards:

- cloud-free or minimal cloud cover;
- late-season imagery to maximize seasonal snow

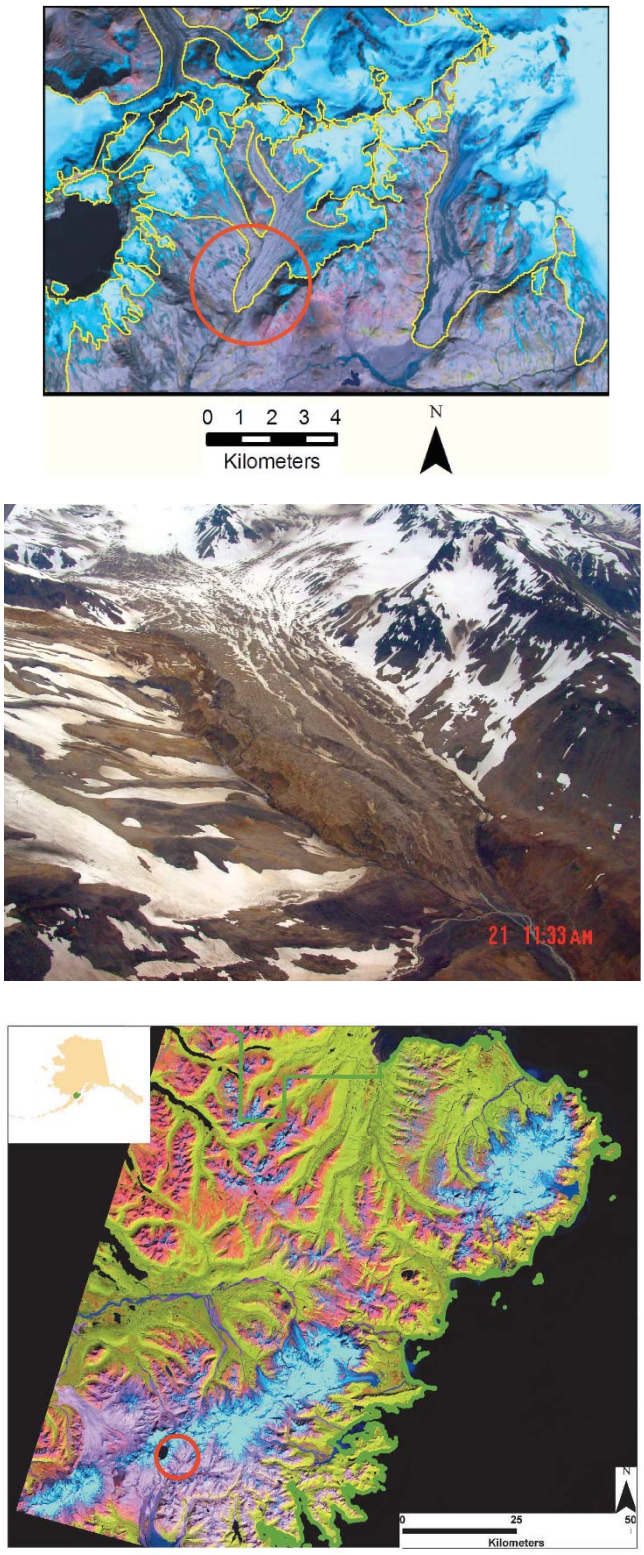

Figure 11.3. Landsat satellite image (Landsat ETM+, August 16, 2000; 542 RGB) of volcanic ash–covered glaciers (top); the yellow line delineates glacier boundaries. Aerial oblique photograph of same volcanic ash–covered glacier (center). Landsat satellite image (Landsat ETM+, August 16, 2000; 542 RGB) showing the position of this glacier in reference to glacierized areas of KATM (bottom).

ablation and minimize new seasonal snow (mid-August through September).

A temporal change detection analysis is performed on a decadal scale using acceptable Landsat imagery. Because of resolution differences between Landsat MSS and Landsat TM/ETM+, the change detection analysis produces accurate results only if the analysis is restricted to the use of Landsat TM and ETM+ imagery.

Glacier mapping in KEFJ was performed using PCI image-processing software. The outlines of the glaciers were traced manually using vector segments to produce vector polygons which were edited further using ArcGIS software. High-resolution (1:65,000 scale) aerial photography (AHAP) was used as a tool to help interpret Landsat data. IKONOS data (2005, 1 m pixel resolution) were also used to interpret selected glacier termini in KEFJ. Very small glaciers and areas that appeared to be snowfields (not glacier ice) were generally not traced. These features are typically small, less than 0.1 km^2.

Glacier mapping in KATM was also performed using PCI image-processing software. However, unlike the work in KEFJ, training sites (glacier areas) were defined and a "maximum likelihood" algorithm was used to classify the imagery. The classification output was converted to GIS shapefile format and edited in ArcGIS.

11.3.2 Complicating issues

There are several issues that influence the accuracy of the initial supervised delineation of glacier extent in both parks including debris-covered ice, shadowing, permanent fields, and seasonal snow cover and/or new snow:

- *Debris-covered ice (moraine and/or volcanic ash)*. Debris-covered ice has a reflectance that is similar to surrounding moraine and/or mountain material (Howarth and Ommanney 1987, Jacobs et al. 1997, Hall et al. 2000, 2003); thus, classification of ice that is completely covered with debris is very difficult and sometimes impossible because its spectral reflectance is very similar to surrounding moraine/mountain material (Williams et al. 1991, Sidjak and Wheate 1999). Some newer approaches are producing useful results (e.g., Kargel et al. 2005, Raup et al. 2007). Manual delineation of multispectral imaging, with topographic data as a guide (e.g., from ASTER DEMs, GDEM, SRTM, or Google Earth), often proves to be the most efficient and reliable method for mapping margins of heavily debris-covered glacier areas.
- *Shadows*. Sun zenith angle and extreme topography are factors affecting the extent of shadowing across an image, which can obscure glacier boundaries.
- *Permanent snowfields outside the accumulation area*. Every effort was made to eliminate permanent and seasonal snowfields from the classification. A snowfield and a glacier are spectrally similar (if the glacier is snow covered), so these two feature types cannot be distinguished using only a single satellite scene. Snowfields attached to glaciers (contributing to glacier ice) were included in the mapping effort. Isolated small snowfield features were not mapped because they do not contribute to glacier ice.
- *Seasonal snow cover and/or new snow cover*. Contrasting a mid-September image with a mid-August image may show significantly less seasonal snow cover, thus increasing the reliability of delineation of the full glacier extent at the time of maximum seasonal ablation. Conversely, early season snowfall may render the mid-September image useless by obscuring the maximum seasonal ablation boundary.

11.3.3 Manual editing

The initial supervised classification was converted to a GIS shapefile format. Areas that were misclassified in the original classification were captured manually (e.g.. debris-covered ice, shadowed ice) or removed (e.g., isolated small snowfields). Editing of the shapefile is based on the experience and judgment of the person doing the satellite image interpretation. The human eye can perceive textural differences in debris-covered ice that are typically missed in the original supervised classification. In addition, local knowledge and the use of high-resolution imagery have aided the interpretation of Landsat data. Careful manual interpretation of these classified areas is required to optimize the accuracy of the mapping effort.

11.4 SATELLITE IMAGERY INTERPRETATION ACCURACY

Park-wide statistics estimating glacier ice extent for both KEFJ and KATM, for each scene studied, were generated using ArcGIS. Also, change

in extent was calculated. The amount of change that can be detected in a Landsat image is dependent on the spatial resolution of the imagery plus any image registration error. The geospatial registration accuracy of terrain corrected TM or ETM+ Landsat data is 30 m between images (EROS Data Center, pers. commun., 2006). If the registration between images is perfect, changes of terminus positions can be determined to within ±42.4 m when analyzing Landsat TM and ETM+ scenes; the accuracy decreases to ±113 m when analyzing data between Landsat MSS and TM or ETM+ scenes (Hall et al., 2003).

11.5 AREAL EXTENT—GLACIER ICE

11.5.1 Kenai Fjords National Park

The areal extent of the Harding Icefield, the Grewingk-Yalik Glacier Complex, and surrounding glaciers was mapped for 1973, 1986, and 2000 using three Landsat scenes (see Table 11.1).

Table 11.2 presents the results of the glacier extent mapping effort for KEFJ. Because of the resolution difference between MSS and TM or ETM+ data, it is difficult to make a quantitative comparison of the 1973 data with the 1986 or 2000 data; thus, 1973 data are not presented in Table 11.2. However, it is reasonable to compare the 1986 and 2000 measurements. A reduction of about 2.2% (−53 km^2) was measured between 1986 and 2000 and is shown in Fig. 11.4 (and Online Supplement 11.3) as a difference map for the Harding Icefield, the Grewingk-Yalik Glacier Complex, and surrounding glaciers.

Table 11.1. Landsat images used in KEFJ.

Date	*Sensor*	*Scene ID number*
17-Aug-73	MSS	LM1074018007322990
12-Sep-86	TM	TM5 LT5069018008625510
9-Aug-00	ETM+	LE7069018000022250

Note that the 2000 image is an early August image and the 1986 image is a mid-September image. One additional month into the melt season for the 1986 image is quite noticeable in terms of the amount of remaining seasonal snow at higher elevations. Though this does not affect the accuracy of the mapping of the terminus positions (lower elevation mapping), it does affect mapping of glacier boundaries and nunataks in higher elevation areas.

11.5.2 Katmai National Park and Preserve

The areal extent of glacier ice in KATM was mapped for 1974, 1987, 1986 (Mt. Martin area

Table 11.2. Summary of the extent of the Harding Icefield, the Grewingk–Yalik Glacier Complex, and surrounding glaciers as measured using Landsat data (in km^2).[a]

	1986 (km^2)	*2000* (km^2)	*1986 to 2000 change in glacier cover* (km^2)	*Change* (%)
Harding Icefield main body[b]	1,828	1,786	−42	−2.3
Harding Icefield and surrounding glaciers	1,935	1,903	−32	−1.7
Grewingk-Yalik Glacier Complex main body	423	412	−11	−2.6
Grewingk-Yalik Glacier Complex and surrounding glaciers	445	424	−21	−4.7
Harding Icefield, Grewingk-Yalik Glacier Complex, and surrounding glaciers	2,380	2,327	−53	−2.2
Glacier ice within park boundary	1,388	1,367	−21	−1.5

[a]This reflects the removal of areas represented by nunataks or other areas barren of glacier ice but inside the mapped boundary of glacier extent.
[b]Aðalgeirsdóttir et al. (1998) state that the extent of the Harding Icefield is ~1,800 km^2.

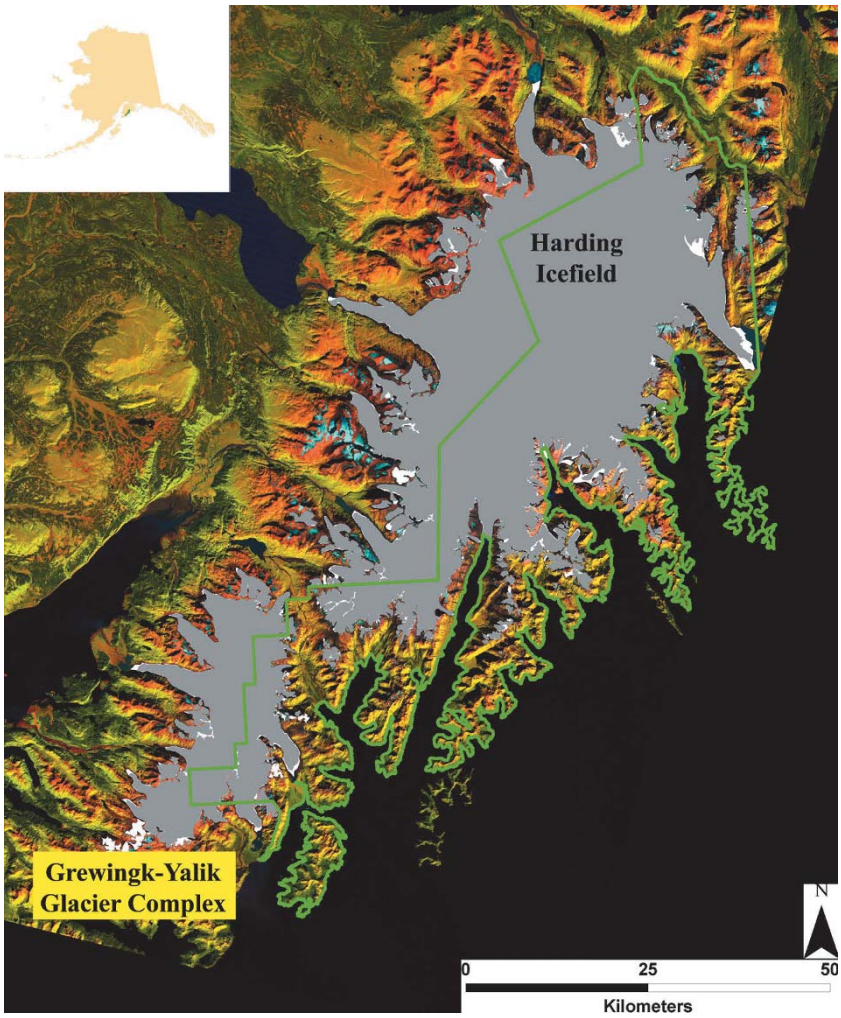

Figure 11.4. Changes in areal extent from 1986 to 2000, Harding Icefield and the Grewingk-Yalik Glacier Complex. White represents the area of glacier ice in 1986 only, and gray represents the area of glacier ice in 2000. The KEFJ boundary is shown in green (Landsat TM5, September 12, 1986; 542 RGB). Figure can also be viewed in higher resolution as Online Supplement 11.3.

only) and 2000, using four Landsat scenes (see Table 11.3).

Table 11.4 presents the results of the glacier extent mapping effort for KATM. Because of resolution differences between the MSS and TM or ETM+ data, it is difficult to make a meaningful comparison of the 1974 data with the 1986/1987 or 2000 data, as discussed previously. Additionally, the 1974 image has more seasonal snow remaining because it was captured earlier in the snowmelt season than the other images. Thus, 1974 data are not presented in Table 11.4. However, comparison of the 1986/1987 and 2000 imagery gives good results. A reduction of about 7.7% (-75 km^2) was measured between 1986/1987 and 2000 and is depicted on a park-wide basis in Fig. 11.5 (and Online Supplement 11.4) as a difference map for the three primary glacierized areas of KATM. It

Table 11.3. Landsat images used in KATM.

Date	*Sensor*	*Scene ID number*
27-Jul-74	MSS	LM1076019007420890
24-Jul-86[a]	TM	LT5071019020086205
21-Aug-87	TM	LT5070018019087233
16-Aug-00	ETM+	L7_P70R19S00_2000AUG16

[a]Mt. Martin area only.

Table 11.4. Summary of the areal extent of glaciers in KATM as measured using Landsat data (in km^2).[a]

	1986/1987 (km^2)	*2000* (km^2)	*1986/1987 to 2000 change in glacier cover* (km^2)	*Change* (%)
Mt. Douglas area	348	330	−18	−5.1
Mt. Katmai, Snowy Mountain, Kukak Volcano area	563	510	−53	−9.4
Mt. Mageik and Mt. Martin	74	70	−4	−5.4
Glacier ice within park boundary	986	910	−76	−7.7

[a]The data above reflect the removal of areas represented by nunataks or other areas barren of glacier ice but inside the mapped boundary of glacier extent.

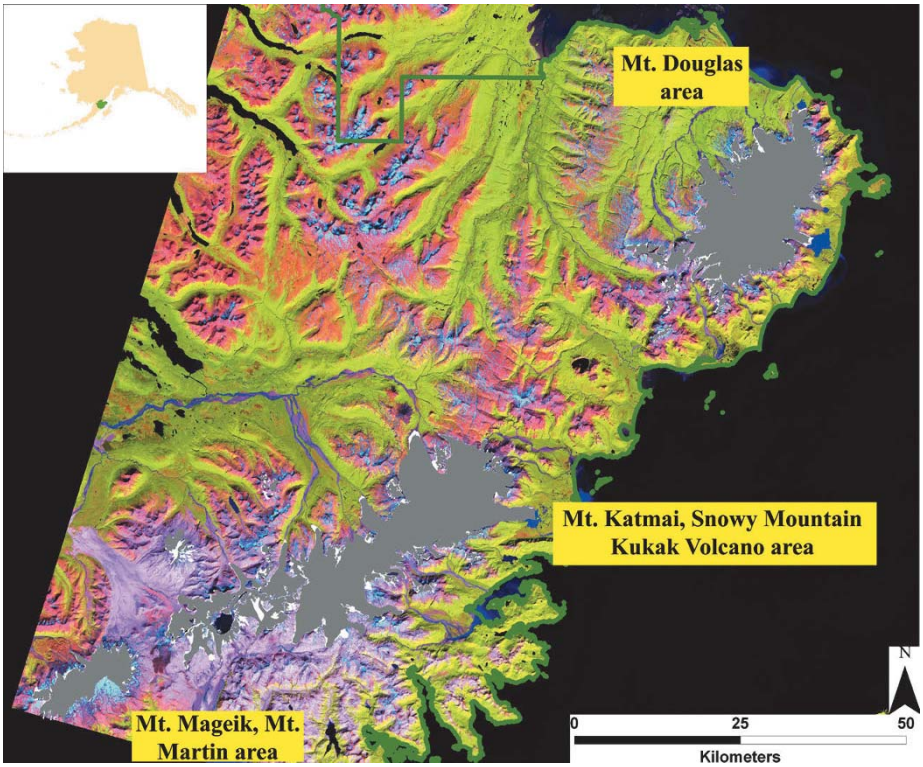

Figure 11.5. Changes in areal extent from 1986/1987 to 2000, KATM. White represents the area of glacier ice in 1986/1987 only, and dark gray represents the area of glacier ice in 2000. A portion of the KATM boundary is shown in green (Landsat ETM+, August 16, 2000; 542 RGB). Figure can also be viewed in higher resolution as Online Supplement 11.4.

is important to note that some of that −7.7% loss is at least in part due to more advanced seasonal snowmelt that is apparent in the 2000 Landsat image as compared with the 1987 Landsat image, thus inflating that amount of observed glacier loss.

11.6 TERMINUS POSITION MEASUREMENTS

11.6.1 Methodology

The glacier terminus "position" can be measured at various points along the terminus of the glacier.

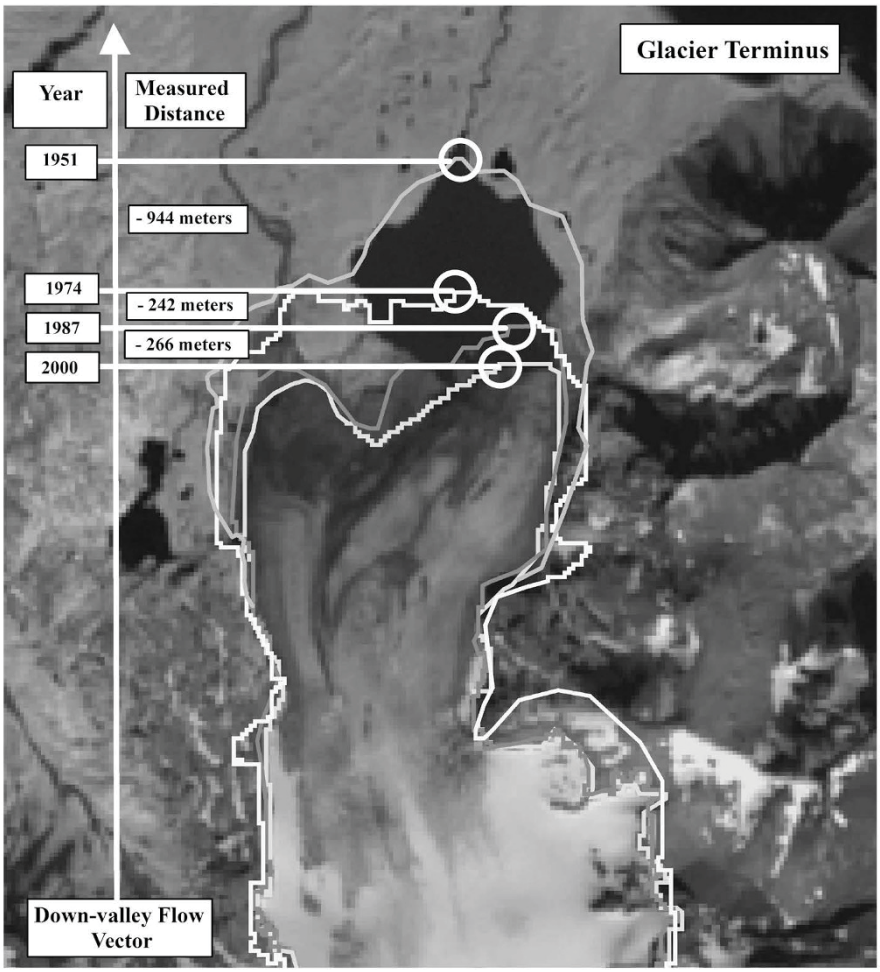

Figure 11.6. Illustration of how glacier terminus position change is measured (Landsat ETM+, August 16, 2000; grayscale).

Changes in terminus positions and rates of recession are approximate because they are highly dependent on the exact spot on the terminus that was selected to make the measurement. For this study, a standard method was developed to select one point on a glacier terminus for each terminus measurement. First, a downvalley vector parallel to the direction of glacier flow was drawn for the glacier. Then the farthest downvalley point on the terminus was identified and a line from this point was projected normal to the downvalley flow vector. The distance between these parallel lines is the distance assigned to the terminus change (Fig. 11.6), which was measured using ArcGIS software.

This analysis shows rates and trends of glacier terminus change, and also identifies which glaciers are most active in terms of terminus change (recession or advancement). The 1951/1952 terminus positions were determined from 15 min USGS quadrangle maps (1:63,360) derived from high-quality aerial photography (scale ca. 1:40,000). Terminus positions from 1986, 1987, 2000, and 2006 (KEFJ only) were determined from Landsat imagery. Terminus positions from 2005 were mapped from IKONOS imagery (KEFJ only). In addition to the use of these data, local knowledge gained through field experience in and around these glaciers and icefields was applied and careful manual interpretation was undertaken to optimize the accuracy of the final product.

11.6.2 Kenai Fjords National Park

The terminus positions were mapped for 27 outlet glaciers emanating from the Harding Icefield and the Grewingk-Yalik Glacier Complex, as shown in Table 11.5. Ten of these glaciers terminate within KEFJ and are marked with a superscript *a* in Table

Table 11.5. Glacier terminus change in KEFJ.

Glacier name	*Change from 1950/1951 to 1986* (m) *Second number is average annual rate of change* (m/yr)		*Change from 1950/1951 to 2000* (m) *Second number is average annual rate of change* (m/yr)		*Change from 1950/51 to 2005/06* (m) *Second number is average annual rate of change* (m/yr)		*Change from 1986 to 2000* (m) *Second number is average annual rate of change* (m/yr)		*Change from 1986 to 2005/2006* (m) *Second number is average annual rate of change* (m/yr)		*Change from 2000 to 2005/2006* (m) *Second number is average annual rate of change* (m/yr)	
Lowell[a]	−741	−21	−1,375	−28	−1,505	−28	−634	−45	−764	−40	−130	−26
A	−586	−17	−906	−18	−1,055	−19	−320	−23	−469	−23	−149	−25
Skilak	−2,267	−65	−4,053	−83	−4,032	−73	−1,786	−128	−1,765	−88	21	4
Killey	−798	−23	−1,229	−25	−1,589	−29	−431	−31	−791	−40	−360	−60
Indian	−692	−20	−973	−20	−1,257	−23	−281	−20	−565	−28	−284	−47
Tustumena	−324	−9	−382	−8	−744	−14	−58	−4	−420	−21	−362	−60
Truuli	−1,065	−30	−971	−20	−1,118	−20	94	7	−53	−3	−147	−25
Chemof	−1,366	−39	−1,461	−30	−1,914	−35	−95	−7	−548	−27	−453	−76
Dinglestadt-west	−2,823	−81	−3,052	−62	−3,408	−62	−229	−16	−585	−29	−356	−59
Kachemak	−801	−23	−989	−20	−1,145	−21	−188	−13	−344	−17	−156	−26
Nuka	−226	−6	−189	−4	−342	−6	37	3	−116	−6	−153	−26
B	−728	−21	−997	−20	−1,115	−20	−269	−19	−387	−19	−118	−20
Dixon	−422	−12	−589	−12	−746	−14	−167	−12	−324	−16	−157	−26
Portlock	−1,188	−34	−1,322	−27	−1,563	−28	−134	−10	−375	−19	−241	−40
Grewingk	−1,350	−39	−2,298	−47	−2,502	−45	−948	−68	−1,152	−58	−204	−34
Wosnesenski	−1,268	−36	−1,436	−29	−1,982	−36	−168	−12	−714	−36	−546	−91
Doroshin	−751	−21	−1,495	−31	−1,644	−30	−744	−53	−893	−45	−149	−25

Petrof	−1,261	−36	−1,576	−32	−1,696	−31	−315	−23	−435	−22	−120	−20
Yalik[a]	−1,057	−30	−1,854	−38	−2,160	−40	−797	−57	−1,103	−58	−306	−61
Dinglestadt-east[a]	−347	−10	−446	−9	−521	−10	−99	−7	−174	−9	−75	−15
McCarty[a]	−1,599	−46	−1,730	−35	−2,248	−42	−131	−9	−649	−34	−518	−104
Northwestern[a]	−5,198	−149	−6,553	−134	−6,367	−118	−1,355	−97	−1,169	−62	186	37
Holgate[a]	−245	−7	−349	−7	−359	−7	−104	−7	−114	−6	−10	−2
Pederson[a]	−706	−20	−860	−18	−1,140	−21	−154	−11	−434	−23	−280	−56
Aialik[a]	186	5	183	4	−105	−2	−3	0	−291	−15	−288	−58
Bear[a]	−158	−5	−1,123	−23	−2,968	−55	−965	−69	−2,810	−148	−1,845	−369
Exit[a]	−488	−14	−481	−10	−621	−12	7	1	−133	−7	−140	−28
Average rate of terminus change	*−1,047*	*−30*	*−1,426*	*−29*	*−1,698*	*−31*	*−379*	*−27*	*−651*	*−33*	*−272*	*−50*
North and west flowing (interior)	−994	−28	−1,344	−27	−1,571	−29	−351	−25	−578	−29	−227	−38
South and east flowing (coastal)	−1,154	−33	−1,590	−32	−1,952	−36	−436	−31	−798	−42	−362	−72

[a] Glaciers that terminate within Kenai Fjords Natioal Park.

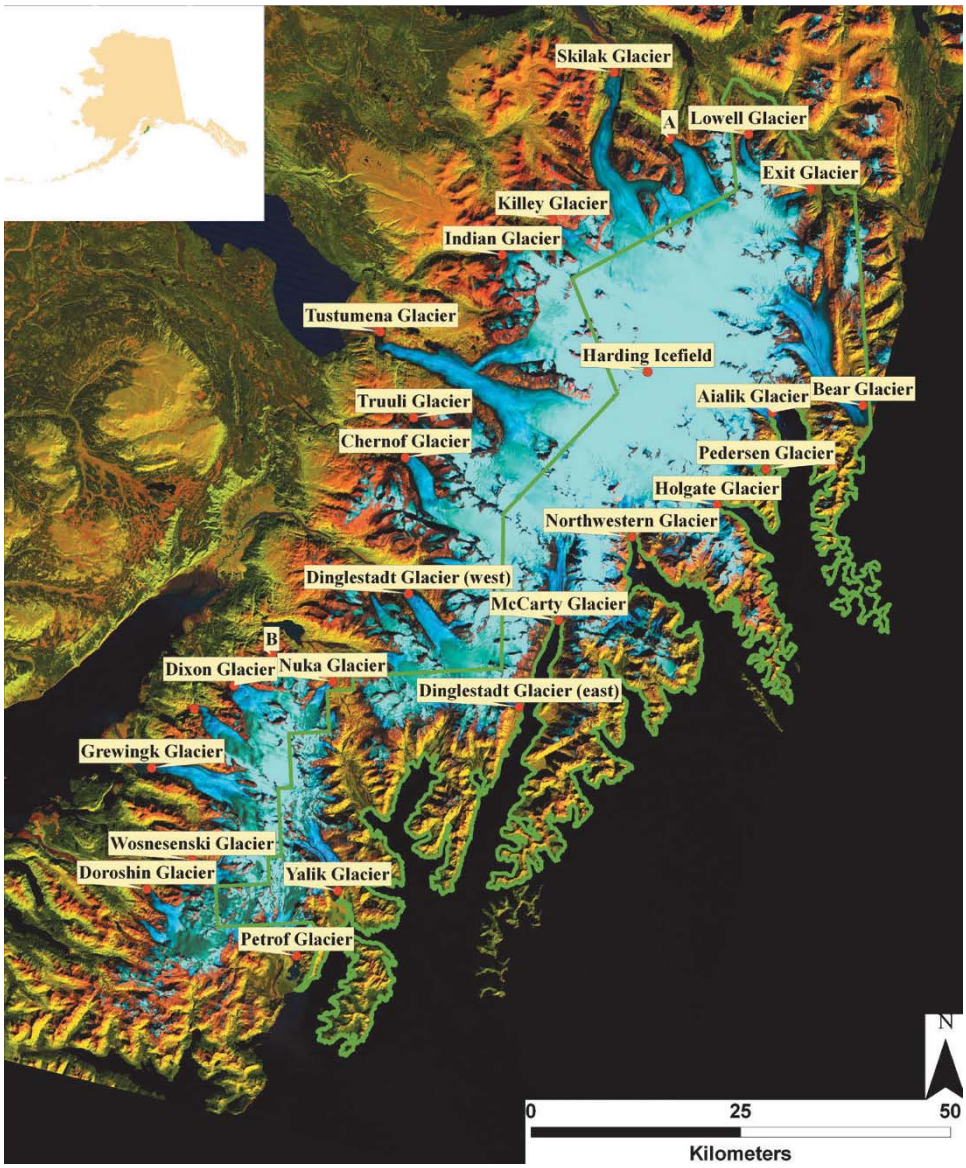

Figure 11.7. Color composite Landsat image of the glacierized portion of KEFJ. The glacier names in this figure identify which glacier termini were measured and correspond to data presented in Table 11.5 (Landsat TM5, September 12, 1986; 542 RGB). Figure can also be viewed as Online Supplement 11.5.

11.5. Fig. 11.7 identifies these glaciers on a Landsat ETM+ image (2000) by name (or alpha code) which corresponds with Table 11.5. Glacier termini positions were mapped using 15 min USGS quadrangles (1950/1951), Landsat TM5 (1986), Landsat ETM+ (2000), IKONOS (2005), and Landsat TM5 (2006) imagery. All 2005 glacier terminus position measurements for glaciers within KEFJ are based on IKONOS imagery. All 2006 glacier terminus positions measurements for glaciers outside KEFJ were mapped from Landsat imagery.

Glacier termini in and around KEFJ have been steadily retreating since the early 1950s (Table 11.5). The rate of recession appears to be slightly higher for tidewater and coastal glaciers (east and south flowing) compared with interior glaciers (north and west flowing). The rates of recession appear to be increasing slightly, though we do not have enough Landsat scenes to confirm this.

There is a dramatic increase in the average rate of recession of glacier termini in KEFJ in the 2000 to 2005 time interval (based on the measurement of

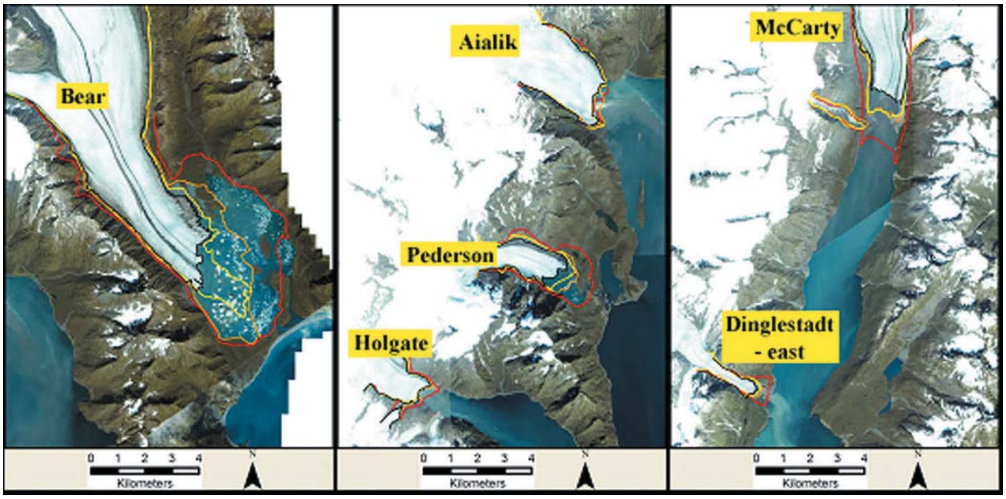

Figure 11.8. Bear Glacier (left); Aialik, Pederson, and Holgate glaciers (center); and McCarty and Dinglestadt glaciers (right)—in KEFJ, Alaska. Glacier terminus positions are shown for 1951 (red), 1986 (orange), 2000 (yellow), and 2005 (black) (GeoEye IKONOS image, 2005).

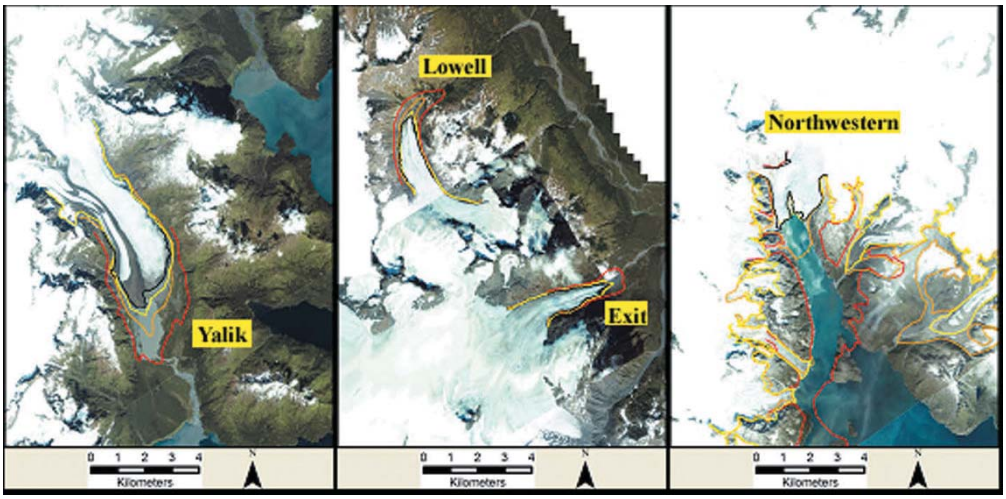

Figure 11.9. Yalik Glacier (left), Lowell and Exit Glaciers (center), and Northwestern Glacier (right)—KEFJ, Alaska. Glacier terminus positions are shown for 1951 (red), 1986 (orange), 2000 (yellow), and 2005 (black) (GeoEye IKONOS image, 2005).

only 10 glaciers). Most of this observed increased rate of recession can be attributed to the collapse of the Bear Glacier terminus during these years.

Terminating in a proglacial lake, Bear Glacier (Fig. 11.8) has experienced disarticulation (Molnia, 2004) where the glacier may have thinned and separated from its terminal moraine, becoming buoyant, and resulting in the observed dramatic retreat from 2000 to 2005. Aialik and Holgate Glaciers show little terminus change since 1951 (Fig. 11.8). Pederson, McCarty and Dinglestadt-east Glaciers all show recession in the 1951 to 2005 time interval, though these glaciers show little terminus change between 1986 to 2000. Yalik, Lowell, and Exit Glaciers all show steady recession from 1951 to 2005 (Fig. 11.9). From Table 11.5, the annual rate of recession for the Yalik, Lowell, and Exit Glaciers has remained fairly consistent throughout the 1951 to 2005 time interval. Northwestern Glacier showed a small advance in the 2000 to 2005 time interval (Table 11.5 and Fig. 11.9).

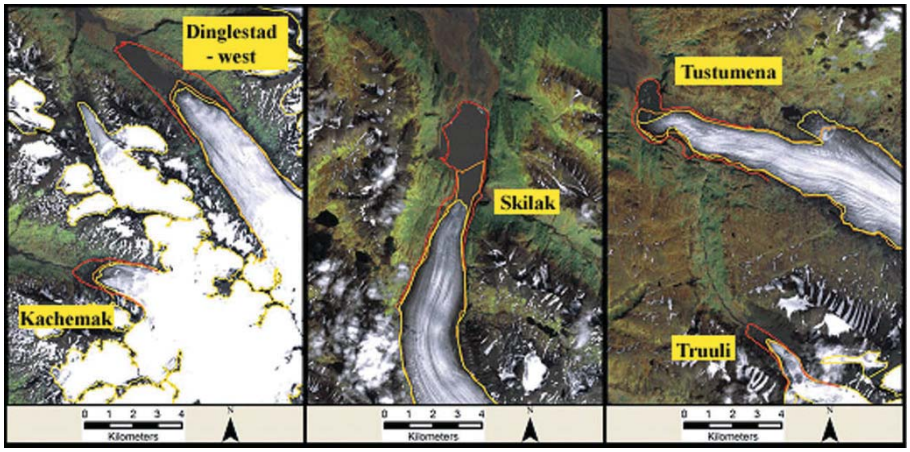

Figure 11.10. Dinglestadt-west and Kachemak Glaciers (left) , Skilak Glacier (center), and Tustumena and Truuli Glaciers (right)—Kenai Peninsula, Alaska. Glacier terminus positions are shown for 1951 (red), 1986 (orange), and 2000 (yellow). The terminus position from 2000 was derived from Landsat ETM+ imagery. Each of these glaciers shows recession from 1951 to 2000 (Landsat ETM+, August 9, 2000; 321 RGB).

Tustumena, Truuli, Skilak, Dinglestadt (west), and Kachemak Glaciers all show recession from 1951 to 2006 (Table 11.5 and Fig. 11.10). The annual rates of recession vary among these glaciers, though Skilak Glacier, terminating in a lake, shows dramatic recession from 1986 to 2000, likely due to disarticulation of the glacier tongue, thus becoming buoyant and breaking up.

11.6.3 Katmai National Park and Preserve

Terminus positions were mapped for 20 glaciers from the three glacierized regions of KATM using the same method as for KEFJ. The results are in Table 11.6. Fig. 11.11 identifies these glaciers on a Landsat ETM+ image (2000) by name (or alpha code) as shown in Table 11.6. Glacier termini were mapped using 15 min USGS quadrangles (1950/1951), Landsat TM5 (1986/1987), and Landsat ETM+ (2000) imagery.

Glacier termini in and around KATM have been retreating since the early 1950s (Table 11.6). The rate of recession on a park-wide basis may be slowing slightly in the most recent study period (1986/1987 to 2000). The rates of recession of interior glaciers (north and west flowing) and coastal glaciers (east and south flowing) are very similar for the 1950s to 1986/1987 time frame. However, in the 1986/1987 to 2000 timeframe, coastal glaciers showed markedly slower rates of recession than did interior glaciers.

Spotted Glacier terminates in a lake (Fig. 11.12), is a north-flowing glacier, and exhibits a consistent rate of recession, though that rate showed a reduction in the 1986/1987 to 2000 time interval. Fourpeaked Glacier, a coastal glacier terminating in a lake (Fig. 11.12), may have become buoyant at the terminus, resulting in a dramatic breakup and retreat sequence in the 1951 to 1986/1987 time interval; recession here has slowed recently (1986/1987 to 2000). Glaciers identified as "B" and "C" (Fig. 11.12) exhibit higher rates of recession during the 1951 to 1986/1987 time interval as compared with the more recent time interval of 1986/1987 to 2000, while glacier "C" has advanced slightly. Glaciers identified as "K" and "L" (Fig. 11.13) exhibit little terminus change during the period (1951 to 2000); this is likely attributable to a thick protective cover of volcanic ash on the surface of these glaciers and shading from extreme topography. Debris cover in excess of 100 mm can act as an insulating layer thus ablation and loss of glacier mass can be significantly reduced (Williams et al. 2002, Adema et al. 2007). Hallo Glacier (Fig. 11.13) may have experienced disarticulation of the terminus, becoming buoyant, and resulting in a rapid breakup and retreat between 1951 and 1986/1987; recession here has slowed, and in the most recent interval (1986/1987 to 2000) Hallo Glacier is one of the rare glaciers in the study area that has advanced slightly. Hook and "H" glaciers exhibit similar recession rates throughout the study period (1951–2000) with rates of recession increasing during the 1986/1987 to 2000 time interval.

Table 11.6. Glacier terminus change in KATM.

Glacier name	*Change from 1951 to 1987* (m) *Second number is average annual rate of change* (m/yr)		*Change from 1951 to 2000* (m) *Second number is average annual rate of change* (m/yr)		*Change from 1987 to 2000* (m) *Second number is average annual rate of change* (m/yr)	
A (Spotted Glacier)	−1,186	−33	−1,452	−30	−266	−20
B	−760	−21	−871	−18	−111	−9
C	−869	−24	−832	−17	37	3
D	−452	−13	−728	−15	−276	−21
E	−383	−11	−511	−10	−128	−10
F (Fourpeaked Glacier)	−3,432	−95	−3595	−73	−163	−13
G (Hook Glacier)	−633	−18	−1,212	−25	−579	−45
H	−632	−18	−1,062	−22	−430	−33
I	−189	−5	−671	−14	−482	−37
J	101	3	−47	−1	−148	−11
K	88	2	69	1	−19	−1
L	108	3	−19	0	−127	−10
M	−541	−15	−615	−13	−74	−6
N	−1,105	−31	−1,357	−28	−252	−19
O	−1,182	−33	−1,298	−26	−116	−9
P (Hallo Glacier)	−916	−25	−766	−16	150	12
Q	−68	−2	−166	−3	−98	−8
R	−432	−12	−735	−15	−303	−23
S (Knife Creek Glacier)	176	5	95	2	−81	−6
T (Serpent's Tongue Glacier)	−1,276	−35	−1,276	−26	0	0
Average rate of terminus change (includes questionable 1972 data)	*−679*	*−19*	*−852*	*−17*	*−173*	*−13*
North and west flowing (interior)	−647	−18	−890	−18	−243	−19
South and east flowing (coastal)	−706	−20	−822	−17	−116	−9

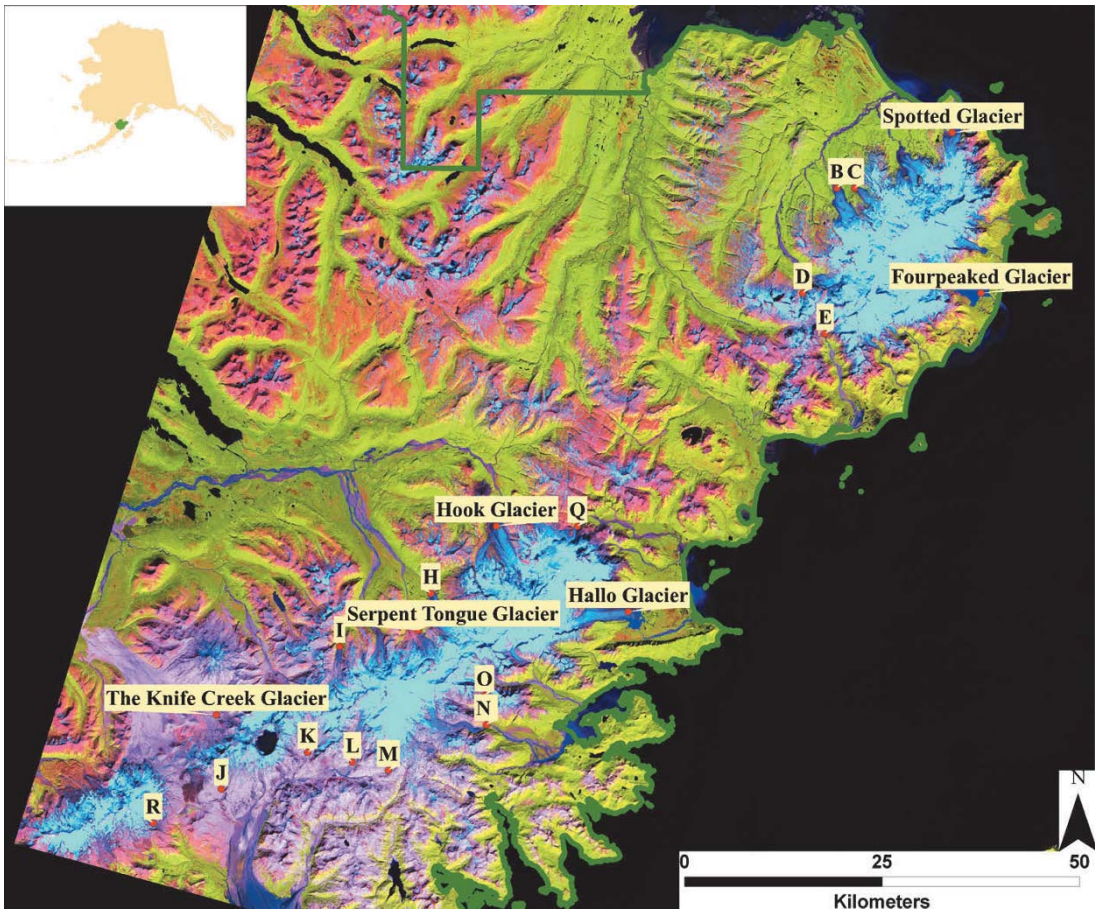

Figure 11.11. Color composite Landsat image of the glacierized portion of KATM. The glacier names (or alpha codes) in this figure identify which glacier termini were measured and correspond to data presented in Table 11.6 (Landsat ETM+, August 16, 2000; 542 RGB). Figure can also be viewed as Online Supplement 11.6.

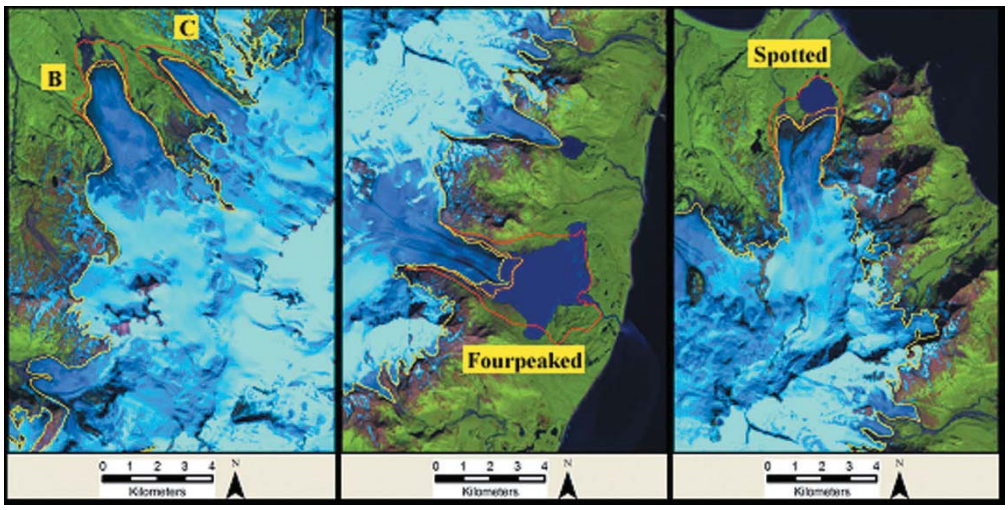

Figure 11.12. ''B'' and ''C'' glaciers (left), Fourpeaked Glacier (center), and Spotted Glacier (right), Katmai National Park and Preserve, Alaska. Glacier terminus positions are shown for 1951 (red), 1987 (orange), and 2000 (yellow). Each of these glaciers shows recession from 1951 to 2000 (Landsat ETM+, August 16, 2000; 542 RGB).

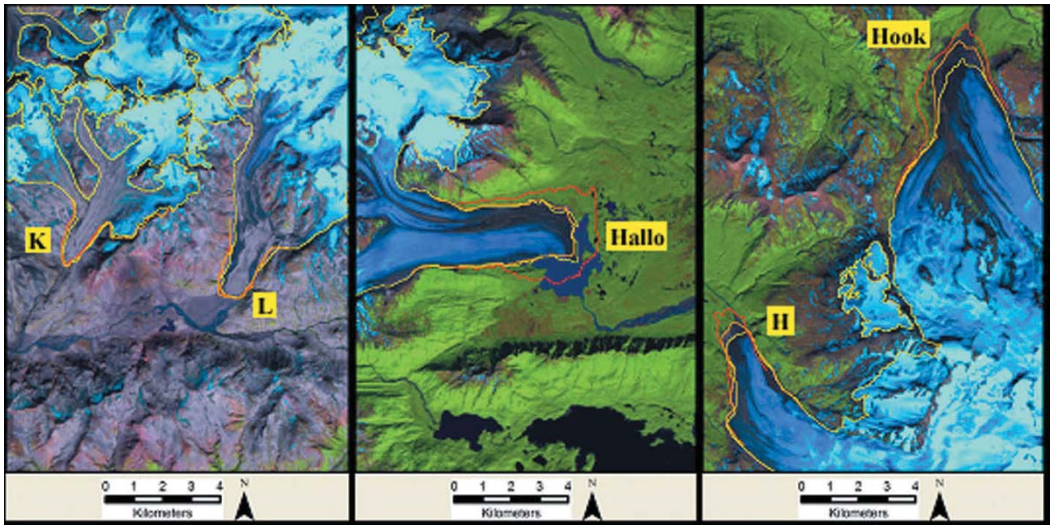

Figure 11.13. ''K'' and ''L'' glaciers (left), Hallo Glacier (center), and Hook and ''H'' glaciers (right), Katmai National Park and Preserve, Alaska. Glacier terminus positions are shown for 1951 (red), 1987 (orange), and 2000 (yellow) (Landsat ETM+, August 16, 2000; 542 RGB).

11.7 DISCUSSION AND CONCLUSIONS

All glacier termini measured in KEFJ have receded, as shown in Table 11.5, between the early 1950s and 2005; some instances of retreat have been dramatic. Two glaciers, Truuli and Nuka, terminating outside the park, show a small amount of advance from 1986 to 2000. Skilak Glacier and Northwestern Glacier are the only two glaciers in the project area exhibiting advance in the 2000 to 2005/2006 period. Land-terminating glaciers have maintained a fairly steady rate of recession of 29 m yr^{-1} through 2000, at which time the average rate of recession jumped to 50 m yr^{-1} in the 2000 to 2005/2006 time interval. Ocean-terminating glaciers have maintained a fairly steady average rate of recession of 32 to 36 m yr^{-1} until 2000, at which time the average rate of recession jumped to 72 m yr^{-1} in the 2000 to 2005 time interval, largely attributable to the dramatic recession of Bear Glacier.

The areal extent of the Harding Icefield, Grewingk-Yalik Glacier Complex, and surrounding glaciers in 1986 and 2000 shows a reduction in area of 53 km^2 or −2.2% (see Table 11.2, Fig. 11.4, and Online Supplement 11.3). Those portions of the Harding Icefield, the Grewingk-Yalik Glacier Complex, and surrounding glaciers within the KEFJ park boundary show a reduction in area of 21 km^2 or −1.5% over the same time interval.

Most glaciers in KATM have receded, as shown in Table 11.6, between the early 1950s and 2000, though several show very little or no change. Glacier termini completely mantled in volcanic ash (Knife Creek Glacier and glaciers ''J'', ''K'', and ''L'') show little change in terminus position over the study period. Fourpeaked Glacier experienced a dramatic recession between the 1950s and 1987. Two glaciers, Hallo and glacier ''C'', show a small amount of advance in the 1987 to 2000 time interval. Interior glaciers have maintained a steady average rate of recession of 18 m yr^{-1} from the 1950s through 2000. Coastal glaciers experienced a rate of recession of 17 m yr^{-1} from the 1950s through 2000 on average. The drop in the average recession rate for coastal glaciers can be attributed to the relative stability of Fourpeaked Glacier's terminus between 1987 and 2000.

The measured area of the three primary glacierized regions in KATM in 1986/1987 and 2000 shows a reduction in area of 76 km^2 or −7.7% (see Table 11.4, Fig. 11.5, and Online Supplement 11.4); at least a portion of this loss is attributable to more advanced seasonal snowmelt observed in the 2000 Landsat image when compared with the 1987 Landsat image.

Due to the remoteness and inaccessibility of most of the glacierized terrain mapped for this project, a thorough error analysis was not performed. However, glacier-mapping efforts in western Canada

using similar glacier boundary–mapping techniques estimated mapping errors of 3–4% (Bolch et al. 2010). These errors arise primarily from lingering seasonal snowpack and debris-covered glacier termini.

Glacier systems of Kenai Fjords National Park and Katmai National Park and Preserve, though both located in southern Alaska and along the Gulf of Alaska coast, appear to be reacting differently during the study period. It is not unusual for glaciers or glacier systems in close proximity to behave and react differently. Some of the features and characteristics that differentiate the glacierized areas of KATM and KEFJ are

- Glacier terminus movement at KEFJ is generally more dynamic than that at KATM. This may be due in part to the fact that KEFJ is both warmer and wetter than KATM. Also, more glaciers terminate in ocean or lake environments in KEFJ than do in KATM. Water-terminating glaciers exhibited more dramatic changes than land-terminating glaciers over the study period.
- Glaciers in KATM lie on steeper terrain and at higher elevations than KEFJ's glaciers. However, based on precipitation models (PRISM), this does not equate to high precipitation rates in KATM. It appears that KATM's cooler and drier conditions (less accumulation, less ablation, less free-flowing water for glacier lubrication) likely retard glacier terminus change as compared with glaciers in KEFJ.

We know that glaciers are undergoing continued recession; however, to fully assess the impact of this recession, measurement of the elevation of the surface of the ice is needed on a repeat basis to calculate glacier volume change. Thus, high-quality digital elevation models (DEM) should be acquired decadally during the August–September time frame.

Mapping of the glacier extent in Lake Clark National Park and Preserve (LACL) is underway, using a similar approach to that described herein. Glacier boundary mapping is completed by using a composite of 1986/1987 Landsat data identifying 2,741 km^2 of glaciers within the park boundary. The 1986 image is an excellent late-season image; however, high-elevation early-season snowfall across the landscape in 1986 required the use of 1987 Landsat data to more accurately record glacier boundaries at higher elevations. The glacier boundary–mapping effort has continued in Lake Clark National Park and Preserve for a recent time period thus allowing for detailed glacier change analysis in this park.

When mapping in LACL is completed, the glacier extent of the three primary glacier parks in the SWAN will be documented for two time periods. GIS shapefiles will be made available to researchers from the Global Land Ice Measurements from Space (GLIMS) project and to other researchers. As a result of careful mapping, as described herein, it will be possible in the future to continue the mapping effort to document changes in glacier ice extent in the SWAN, thus facilitating land cover and climate studies with a high degree of accuracy. In addition, in conjunction with surface elevation measurements, it will be possible to determine changes in the volume of ice in the SWAN.

11.8 REFERENCES

Aðalgeirsdóttir, G., Echelmeyer, K.A., and Harrison, W.D. (1998) Elevation and volume changes on the Harding Icefield, Alaska. *Journal of Glaciology*, **44**(148), 570–582.

Adema, G.W., Karpilo, R.D., and Molnia, B.F. (2007) Melting Denali: Effects of climate change on the glaciers of Denali National Park and Preserve. *Alaska Park Science*, **6**(1), 13–17.

Arendt, A.A., Echelmeyer, K.A., Harrison, C.A., Lingle, C.A., and Valentine, V.B. (2002) Rapid wastage of Alaska glaciers and their contribution to rising sea level. *Science*, **297**, 382–386.

Bennett, A., Thompson, B., and Mortenson, D. (2006) *Vital Signs Monitoring Plan Southwest Alaska Network Inventory and Monitoring Program*, U.S. National Park Service, Anchorage, AK, 223 pp.

Bolch, T., Menounos, B., and Wheate, R. (2010) Landsat-based Inventory of Glaciers in Western Canada, 1985–2005. *Remote Sensing of Environment*, **114**(2010), 127–137.

Daly, C., Neilson, R.P., and Phillips, D.L. (1994) A statistical–topographic model for mapping climatological precipitation over mountainous terrain. *Journal of Applied Meteorology*, **33**, 140-158.

Daly, C., Gibson, W.P., Taylor, G.H., Johnson, G.L., and Pasteris, P. (2002) A knowledge-based approach to the statistical mapping of climate. *Climate Research*, **22**, 99–113.

Davey, C.A., Redmond, K.T., and Simeral, D.B. (2007) *Weather and Climate Inventory* (National Park Service, Southwest Alaska Network, WRCC Report 2007-20), Western Regional Climate Center, Desert Research Institute, Reno, NV, 96 pp.

Dyurgerov, M., and Meier, M. (1997) Mass balance of mountain and subpolar glaciers: A new global assessment for 1961–1990. *Arctic and Alpine Research*, **2**(4), 379–391.

Echelmeyer, K.A., Harrison, W.D., Larsen, C.F., Sapiano, J., Mitchell, J.E., DeMallie, J., Rabus, B., Adalgeirsdóttir, G., and Sombardier, L. (1996) Airborne surface profiling of glaciers: A case-study in Alaska. *Journal of Glaciology*, **42**(142), 538–547.

Field, W.O. (Ed.) (1975) *Mountain Glaciers of the Northern Hemisphere*, Vols. 1 and 2, Cold Regions Research and Engineering Laboratory, Hanover, NH.

Hall, D.K., Williams, R.S., Jr., Barton, J.S., Sigurdsson, O., Smith, L.C., and Garvin, J.B. (2000) Evaluation of remote-sensing techniques to measure decadal-scale changes of Hofsjökull ice cap, Iceland. *Journal of Glaciology*, **46**(154), 375–388.

Hall, D.K., Bayr, K.J., Schöner, W., Bindschadler, R.A., and Chien, J.Y.L. (2003) Consideration of errors inherent in mapping historical glacier positions in Austria from the ground and space (1893–2001). *Remote Sensing of Environment*, **86**, 566–577.

Hall, D.K., Giffen, B.A., and Chien, J.Y.L. (2005) Changes in the Harding Icefield and the Grewingk-Yalik Glacier Complex. Paper presented at *Proceedings of the 62nd Eastern Snow Conference, Waterloo, ON, Canada*, pp. 29–40.

Howarth, P., and Ommanney, C.S. (1987) The use of Landsat digital data for glacier inventories. *Annals of Glaciology*, **8**, 90–92.

Jacobs, J.D., Simms, E.L., and Simms, A. (1997) Recession of the southern part of Barnes Ice Cap, Baffin Island, Canada, between 1961 and 1993, determined from digital mapping of Landsat TM. *Journal of Glaciology*, **43**(143), 98–102.

Kargel, J.S., Abrams, M.J., Bishop, M.P., Bush, A., Hamilton, G., Jiskoot, H., Kääb, A., Kieffer, H.H., Lee, E.M., Paul, F. et al. (2005) Multispectral imaging contributions to Global Land Ice Measurements from Space. *Remote Sensing of Environment*, **99**, 187–219.

Meier, M., and Post, A. (1987) Fast tidewater glaciers. *Journal of Geophysical Research*, **92**, 9051–9058.

Molnia, B.F. (2004) *Glossary of Glacier Terminology: A Glossary Providing the Vocabulary Necessary to Understand Modern Glacier Environment* (USGS Open File Report 2004-1216), U.S. Geological Survey, Reston, VA.

Motyka, R.J. (1977) *Katmai Caldera: Glacier Growth, Lake Rise and Geothermal Activity* (Geologic Report No. 55), State of Alaska, Department of Natural Resources, Anchorage, AK, pp. 17–21.

Raup, R., Kääb, A., Kargel, J.S., Bishop, M.P., Hamilton, G., Lee, E., Paul, F., Rau, F., Soltesz, D., Khalsa, S.J.S. et al. (2007) Remote sensing and GIS technology in the Global Land Ice Measurements from Space (GLIMS) project. *Computers and Geoscience*, doi: 10.1016/j.cageo.2006.05.015.

Sapiano, J.J., Harrison, W.D., and Echelmeyer, K.A. (1998) Elevation, volume and terminus changes of nine glaciers in North America. *Journal of Glaciology*, **44**(146), 119–135.

Sidjak, R.W., and Wheate, R.D. (1999) Glacier mapping of Illecillewaet Icefield, British Columbia, Canada, using Landsat TM and digital elevation data. *International Journal of Remote Sensing*, **20**(2), 273–284.

Wiles, G.C. (1992) Holocene glacial fluctuations in the southern Kenai Mountains, Alaska. Thesis, University of New York-Buffalo, 333 pp.

Williams, R.S., Jr., and Ferrigno, J.G. (2002) *Satellite Image Altas of the Glaciers of the World—North America* (USGS Professional Paper 1386J), U.S. Geological Survey, Reston, VA, p. J354.

Williams, R.S., Jr., Hall, D.K., and Benson, C.S. (1991) Analysis of glacier facies using satellite techniques. *Journal of Glaciology*, **37**, 120–128.